Efficient high-precision CCD-field lens alignment and integration process of mass-produced fast astronomical spectrograph cameras with VIRUS as an example

Lee, Hanshin, Vattiat, Brian, Hill, Gary

Hanshin Lee, Brian L. Vattiat, Gary J. Hill, "Efficient high-precision CCD-field lens alignment and integration process of mass-produced fast astronomical spectrograph cameras with VIRUS as an example," Proc. SPIE 10706, Advances in Optical and Mechanical Technologies for Telescopes and Instrumentation III, 107061K (10 July 2018); doi: 10.1117/12.2314638

SPIE.

Event: SPIE Astronomical Telescopes + Instrumentation, 2018, Austin, Texas, United States

Efficient high-precision CCD – field lens alignment and integration process of mass-produced fast astronomical spectrograph cameras with VIRUS as an example

Hanshin Lee, Brian L. Vattiat, Gary J. Hill,
McDonald Observatory, University of Texas at Austin, 2515 Speedway, C1402, Austin, TX, USA 78712-0259

ABSTRACT

Spectrographs in high-multiplex fiber integral-field spectroscopy tend to have fast large field-of-view camera systems in order to meet the desire of packing as many spatial elements and wide a spectral bandpass as possible, thereby maximizing the use of detector real estate. This, very often, leads to a camera design with a field flattening lens very close to the detector active area with tight tolerances in the relative alignment between those two, on the order of a few hundredths of a degree and millimeter. This requires dedicated optical metrology process, particularly in cases where a large number of spectrographs, on the order of 100 or more, need to be accurately and reliably aligned and integrated. We have developed such a metrology process for the 156 camera systems in the VIRUS instrument. We detail the working principle of this metrology process, the implementation for the VIRUS camera systems, and how it can be applicable to multi-lens camera system alignment and integration.

Keywords: CCD-Field lens, Fast Spectrograph Camera, Alignment, VIRUS

1. INTRODUCTION

High-multiplex astronomical fiber-fed integral-field spectroscopy over wide fields is becoming an important and powerful tool for understanding various astrophysical phenomena. Spectrographs used in such observing tend to have high numerical-aperture large field-of-view camera systems in order to meet the desire of packing as many spatial elements and as wide a spectral bandpass as possible per spectrograph, thereby maximizing use of detector real estate. This, very often, leads to a camera design with a field flattening lens very close to the detector active area with tight tolerances in the relative alignment between those two, on the order of a few hundredths of a degree and millimeter. Alignment to this level of accuracy requires dedicated optical and mechanical metrology setups and process, particularly in situations where the number of spectrographs is high, on the order of 100 or more, and therefore accurate and repeatable results are highly desired.

We have developed such a metrology process for the camera systems in the VIRUS instrument. The metrology consists of two parts. In one part, the field flattening lens is aligned in centration and tilt and integrated to a fiducial target by locating the optical conjugate points of the lens using an auto-collimating alignment telescope. In the second part, a CCD is aligned and integrated with respect to the same fiducial target by using the same alignment telescope on a linear translation stage to locate fiducial marks on the CCD. The two components are assembled after these processes, with their final integrated alignment meeting the required tolerances. This process uses a common fiducial target for alignment registration and eliminates the need for a rotary stage often used in centering lenses. This process is in principle applicable to other types of alignment and integration of multi-lens systems. We detail the working principle of this metrology process,

Advances in Optical and Mechanical Technologies for Telescopes and Instrumentation III, edited by Ramón Navarro, Roland Geyl, Proc. of SPIE Vol. 10706, 107061K · © 2018 SPIE
CCC code: 0277-786X/18/$18 · doi: 10.1117/12.2314638

the implementation and result for the VIRUS camera systems, and how it can be further extended to multi-lens camera system alignment and integration.

2. CONTEXT

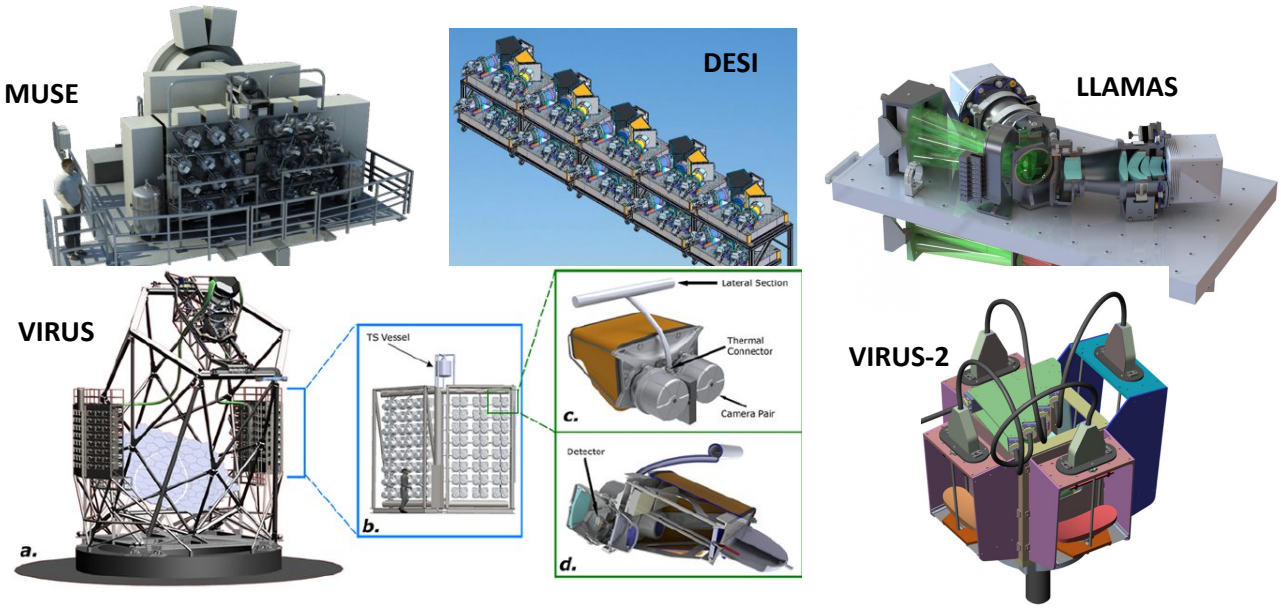

Figure 1 Example high-multiplex replicated astronomical spectrographs[1][2][3][4][5].

We are witnessing many high-multiplex replicated astronomical spectrographs in operation, coming on-line , or under development (Figure 1)[1][2][3][4][5]. These spectrographs are becoming powerful and effective tools for targeted and/or blind surveys of astronomical objects over different physical scales. These are quite different from traditional monolithic instruments built in 80s and 90s. And it is widely recognized that the birth of such replicated spectrographs has been made possible by the modern standard precision mass-production capabilities in high performance optical, mechanical, and electrical components at significantly lower cost than before. Currently, however, some of the components needed in astronomical spectrographs are manufactured by processes that include several “custom” aspects and hence a small increase in the unit cost may blow up the entire instrument cost, making a replicated instrumentation approach infeasible. Particularly, the optical glass material and detector system are considered such components. For example, spectrograph systems based on large (> 250mm in diameter) glass can place a significant constraint in the types of available glasses, frequencies of glass fabrications, and ultimately cost and schedule. An additional challenge could be seen in fabricating diffraction gratings in large format. The detector system occupies the most significant portion of the overall budget for most of astronomical spectrograph instruments. It is important to carefully analyze the cost implications of these components in the context of the overall instrument budget and thus one must go through a quite extensive trade-off study to come up with a reasonable solution for the instrument architecture and the overall budget. This is becoming more crucial than ever in the era of reduced public funding for building astronomical instruments.

For cost effective optical systems, keeping the overall size of optics as much as possible is the key. At the same time, it is quite necessary to design optical systems in such a way that one can utilize the detector real-estate most effectively, by placing more spaxels over the given number of pixels of a detector system. These two effects tend to nudge the camera design of a spectrograph system toward a short focal length (~ 100mm) and wide-field of view (~ 25deg) camera with very high numerical aperture (~ f/1). The tendency of

such a camera design is that the camera alignment and integration tolerances, especially the relative alignment between the detector and the field flattening lens, become quite tight. In addition, since one must repeat such alignment and integration processes multiple times (potentially more than 100 times), it becomes extremely important that such camera alignment and integration can be performed in a time-efficient, straight-forward, deterministic, and repeatable manner. With this context in mind, we are presenting some details of the conjugate point matching technique we used for aligning/integrating the VIRUS[1] CCD and field flattening lenses.

3. HETDEX AND HET WIDE-FIELD UPGRADE

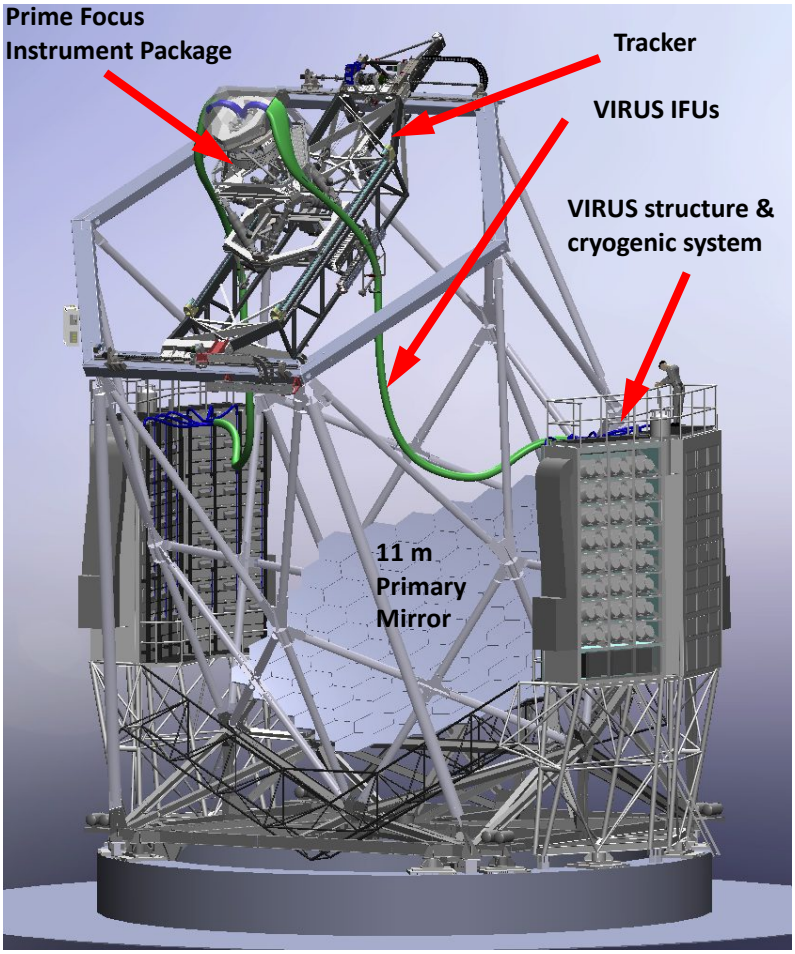

Figure 2 The upgraded Hobby-Eberly Telescope with the new top-end tracker, wide-field corrector, and prime-focus instrument package and the 150+ channel VIRUS spectrographs on each side of the telescope.

Before diving into the details of the VIRUS CCD and field lens alignment / integration, let us briefly touch on the HETDEX (Hobby-Eberly Telescope Dark Energy Experiment) and the HET Wide-field Upgrade[6][7]. The HETDEX is a multi-year-long wide-field survey of the Lyman-α galaxies in the redshift region between 2.5 and 3.5, which corresponds to 9 to 11 billion light years in look back time. The survey will result in a 3-dimensional map of these galaxies (one million in numbers). The survey data will allow astronomers to make an accurate measure of how fast the universe is expanding at different times in its history, which will provide a constraint

on the characteristics of Dark Energy and can give us a discriminant with which astronomer can eliminate some of the competing ideas on Dark Energy.

The Wide-field Upgrade consists of two parts (Figure 2). The first part is to upgrade the HET's top end consisting of the tracker system, the wide-field corrector[8], and the prime-focus instrument package[9][10]. These upgrades, already completed, transformed the HET into much more stable and precise (~μm positioning over 7m range) and high-performance 10m-aperture imaging camera with 25 times wider instantaneous field in area (22arcmin in diameter) than the previous HET. The second part of the upgrade is the VIRUS instrument, which consists of 156 channels of astronomical spectrographs fed by 35,000 fiber optics in the form of 75 Integral-Field Units (green cables in Figure 2) and the main facility to be used in the HETDEX survey. In addition to the VIRUS instrument, there is the second-generation low-resolution spectrograph (LRS-2)[11][12][13] and the near-infrared Habitable-zone Planet Finder (HPF) instrument [14]current in science operations. The facility optical high-resolution spectrograph (HRS) is current undergoing a significant make-over and will be available later. More detailed information on the new HET and its instruments can be found from [6].

4. VIRUS SPECTROGRAPH

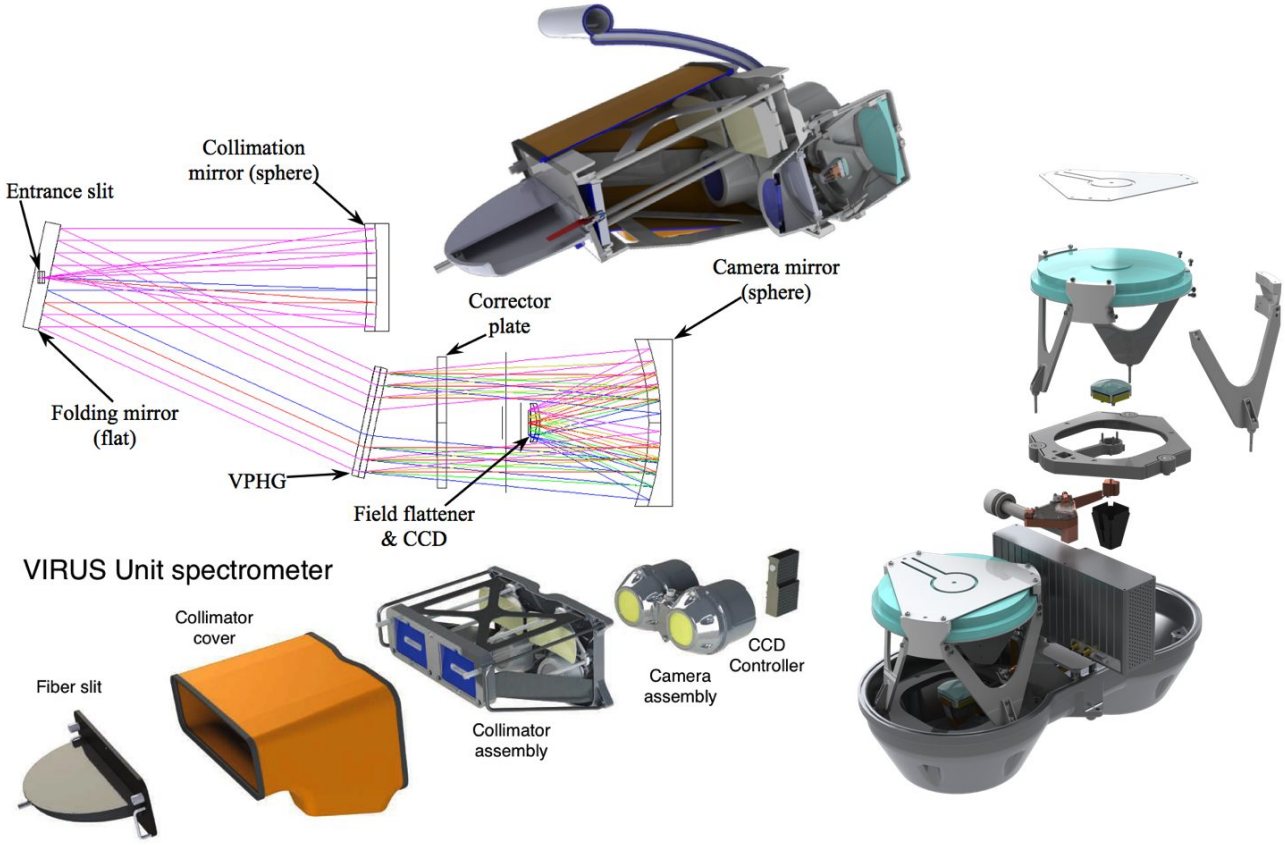

Figure 3 Various views of the VIRUS Spectrograph[1].

Figure 3 shows various views of the VIRUS spectrograph. The telescope beam, having propagated through the IFU fiber cables, diverges out of the fiber slit into each spectrograph channel. The beam is then collimated by the spherical collimation mirror and propagates to the diffraction grating through a reflection off the folding flat mirror. Each channel is equipped with a volume phase holographic grating (VPHG) that diffracts the

collimated beam into wavelength components between 350nm and 550nm. The VIRUS spectrograph camera is based on the Schmidt design where the dispersed spectrum is imaged onto a CCD through reflections and refractions of the Schmidt camera mirror, corrector lens, and field flattening lens. An exploded view of the VIRUS spectrograph assembly as well as of the Camera cryostat is shown.

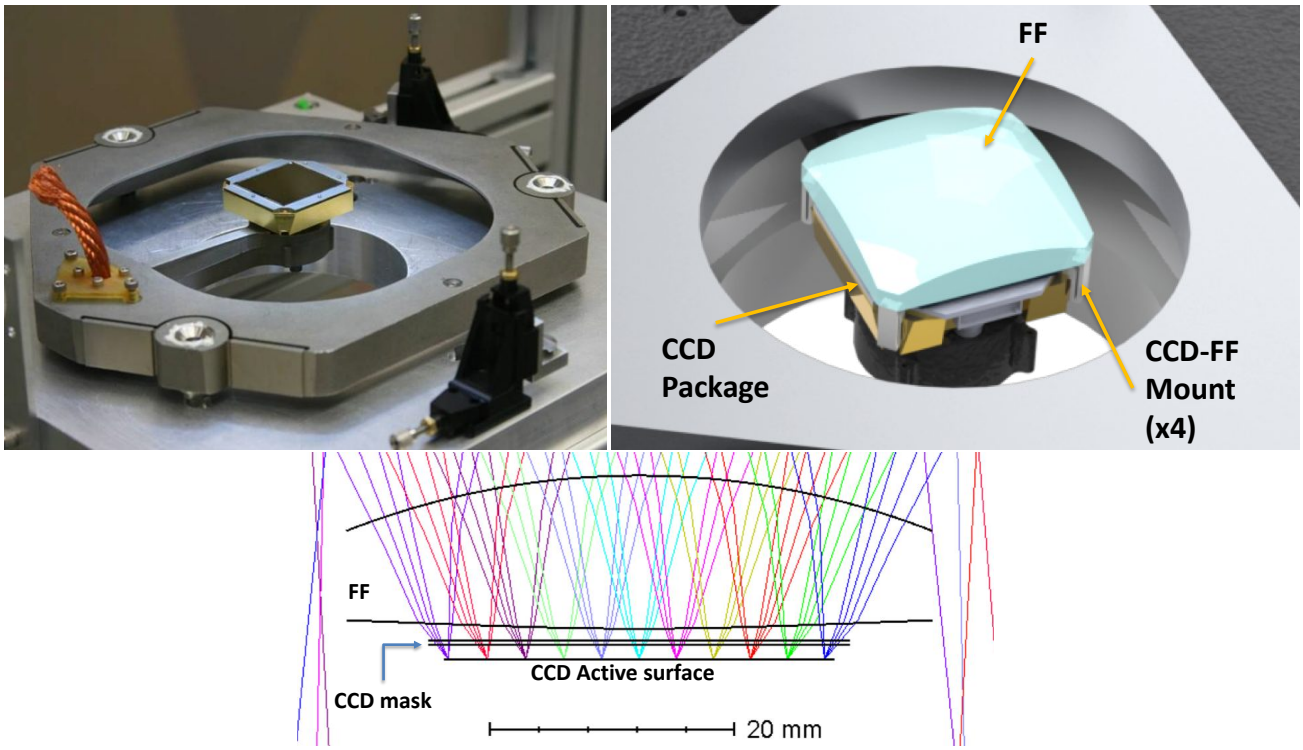

Figure 4 Example views of the VIRUS CCD and Field flattener package.

Figure 4 shows close-up views of the VIRUS CCD and Field lens. The CCD package is mounted to an invar spider which kinematically interfaces to the cryostat body at three places. The field lens is bonded to its mount at four corners and the field lens mount is clipped and fastened into the CCD invar substrate at three corners out. The leg at the unfastened corner is ground to a shorter length and does not touch the CCD substrate. As shown in the optical ray diagram, the field lens is extremely close to the CCD active surface. The center distance between two elements is 2.5mm. The challenge is to align the field lens to the CCD to the accuracy of ±100µm in centration, ±50µm in focus, ±50mdeg in tip/tilt, and ±30mdeg in clocking angle[15].

In order to align and integrate the CCD and field lens to the prescribed accuracy, we have developed the following procedure as illustrated in Figure 5. The field lens is aligned and then integrated into its mount independently with respect to the surrogate CCD substrate. The CCD is independently aligned and then integrated into its spider mount with respect to the surrogate kinematic mounting mounts of the cryostat. Finally, the field lens on its mount is integrated into the CCD package. The CCD and field lens integration / alignment happens in separate stations and can be parallel to each other if needed. Also note that the height of the field lens and CCD is controlled by using a touch probe micrometer. This is shown as the height probe in the illustration. During the alignment, the field lens and CCD are sitting on separate 6DOF adjustment mechanisms (which is represented by spring coils in the diagram). The touch probes are set to zero with respect to the pre-determined datum surface before the alignment starts and the difference between this

datum height and the actual measured surface (i.e. the back surface of the field lens and the CCD substrate) is minimized as the alignment process progresses.

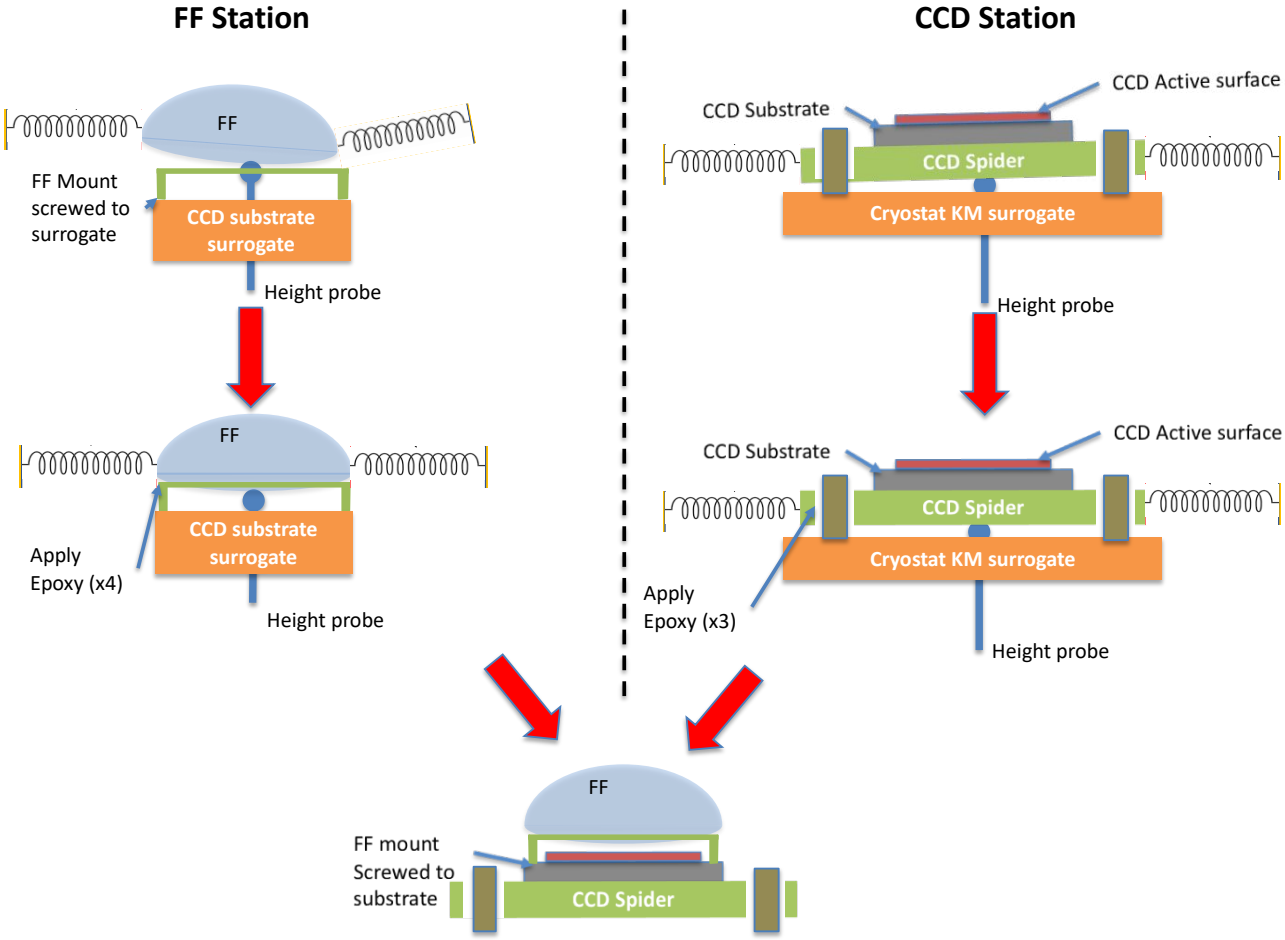

Figure 5 An illustration of the VIRUS CCD – field lens integration and alignment procedure. The spring coils represent adjustment mechanisms in 6 degrees of freedom.

5. ALIGNMENT METROLOGY VIA CONJUGATE POINT MATCHING

5.1. Principles of operation

In order to make the CCD – field lens alignment / integration procedure straightforward and deterministic, we adopted a metrology technique called the conjugate point matching (CPM) as illustrated in Figure 6. On the left, the field lens alignment metrology is shown. Some of the commercial alignment telescopes, such as D275 from Davidson Optronics, provides a way to project the internal reticle target onto surfaces at different distances along the optical axis of the alignment telescope. When the field lens is placed between one of the conjugate point and the alignment telescope, it is possible for match the conjugate point of the alignment telescope to those of the field lens surfaces. For example, the alignment telescope can be adjusted to place its conjugate point roughly a few inches from the front surface of the field lens. This point is where the back surface of the field lens is located and thus the beam from the alignment telescope returns back to itself along

the same optical path. The same can be done for the front surface, where the alignment telescope is now conjugate to the front surface conjugate point a few mm below the field lens. At each conjugate point, the alignment telescope provides the returned target image that is shifted in x and y axes by varying amounts. And this shift is related to the centration and tilt alignment error of the field lens. Since there are 4 shift measurements from 2 surfaces, it is possible to construct a 4x4 matrix equation to uniquely determine the two centration parameters as well as two tilt parameters of the field lens with respect to the alignment telescope. This matrix equation can either be theoretically constructed by using the knowledge of where the field lens is roughly located with respect to the alignment telescope or empirically built by measuring the sensitivities of the measured shifts to each of the field lens degrees of freedom. Since the field lens surfaces are rotationally symmetric, we do not constrain the lens' clocking angle during the alignment. The same procedure can be applied to the CCD, where the conjugate points are at infinity for tilt measurement and at the CCD substrate for centering/clocking measurement. Note that the focus parameter is constrained by the linear touch probe.

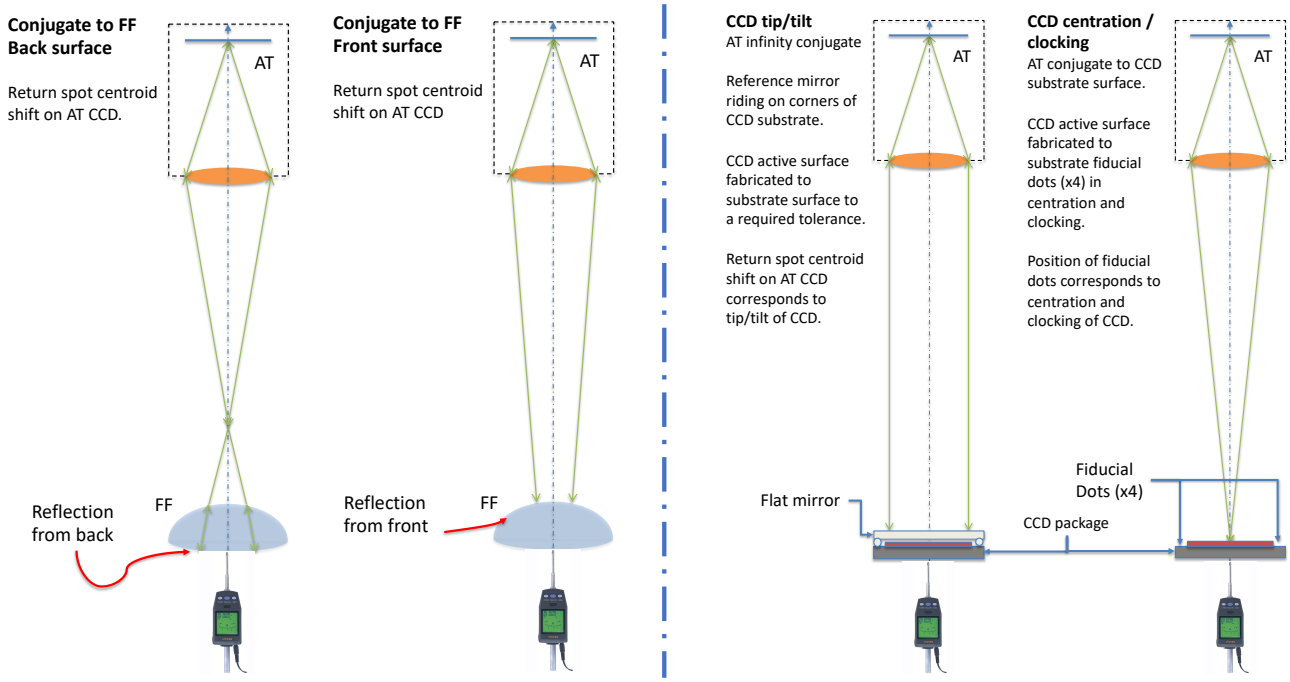

Figure 6 Illustrations of the Conjugate Point Matching process for the field lens (Left) and the CCD (Right).

5.2. Apparatus

Figure 7 shows a picture of the CCD and field lens metrology station. Each station has a D-275 alignment telescope that is retrofitted with a machine vision CCD camera. To illuminate the internal reticle target of each alignment telescope, we supply LED light through a liquid light guide into the existing lamp port of the alignment telescope. Each D-275 is mounted onto 6DOF mechanism so that it can be aligned to datum targets before the alignment starts. In this way, we are essentially transferring the datum to the alignment telescope using the shift in the returned reticle images. The 6DOF mechanisms of the D-275 in the CCD station are motorized and encoded by linear touch probe in X/Y translation axes. This is due to the fact that the D-275 working distance to the CCD is set to the optimal distance for the image sampling and space constraint. This resulted in the field of view of the D-275 much smaller than the CCD substrate size. Hence it was necessary to translate the D-275 in X/Y axes to access the fiducial features on the CCD substrate for constraining the

centration and clocking of the CCD. The repeatability of the X/Y stage over the CCD substrate area is roughly a couple μm and the tilt angle change over this distance against a flat mirror was measured to be about sub arcseconds. Near the bottom of each station, there is an alignment platform. This is where the field lens or CCD are mounted to 6DOF adjustment mechanisms and aligned/integrated into its respective packages/mounts. Underneath this alignment platform, there is a linear touch probe for focus measurements.

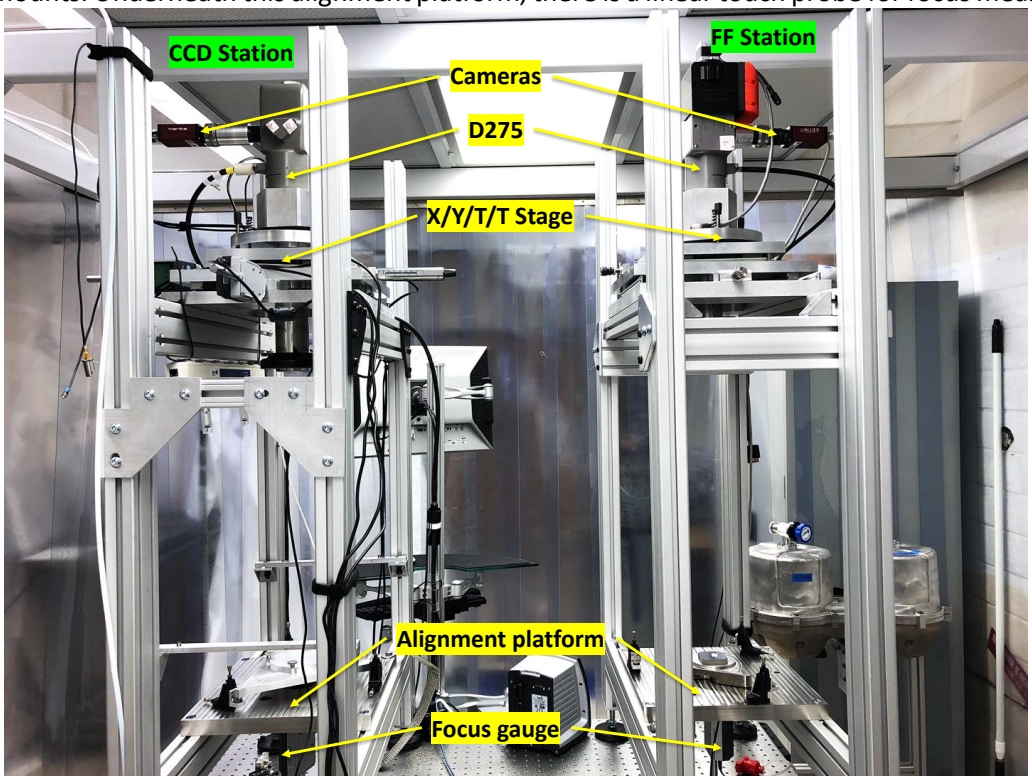

Figure 7 A view of the CCD (Left) and field lens (Right) metrology stations.

Figure 8 shows the view of the alignment platform. What is depicted is the CCD-field lens integrated onto the spider mount which is connected to a triangular plate on the 6DOF adjustment mechanism. Note three kinematic bushings on the (black) spider mount which are bolted to the alignment platform in three places. There are gaps between these bushings and the spider so that once the alignment of the CCD is complete, the gaps are filled with vacuum epoxy. The 6DOF adjustment mechanism consists of 6 independent linear manual adjusters. The triangular plate has features specific to either the field lens or CCD to allow the part to be adjusted by the adjustment mechanism. For example, the triangular plate for the CCD has 3 thru-holes to allow the spider to be fastened to the plate for the alignment.

For the alignment / integration process to be successful, it is crucial for us to be able to set the datum reference for each DOF of the field lens and the CCD. We adopted a method where we build precision datum fixtures to which the alignment telescopes are registered. This is essentially equivalent to transferring the datum to the alignment telescopes and use them as the reference for aligning the field lens and CCD. Figure 9 shows a few pictures of the datum fixtures for the field lens and example images of the D-275 reticle target images through these fixtures. The triangular fixture with fine ground flat top mimics the CCD substrate surface and contains the same key features of the CCD substrate. The center hole with conical edge allows us to place a precision tooling ball so that the center of the surrogate CCD substrate surface can be located. The top right image corresponds to the reticle target image when the D-275 is conjugate to the center of the tooling ball. The surrounding area is visible through the reflection from the ball. The same reference mirror

can be placed on the surrogate surface to set the tilt datum for the field lens and bottom right image shows the returned reticle target through the reflection from the mirror.

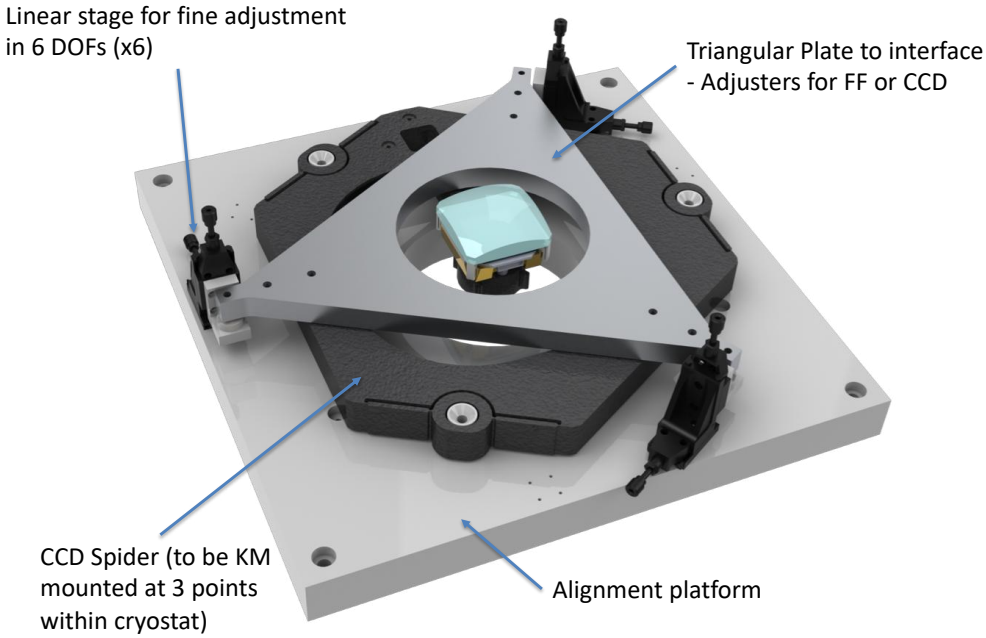

Figure 8 The 6DOF adjustment mechanism for the field lens and CCD. What is shown is the CCD-field lens package on the spider mount that is attached to the triangular plate for adjustment. The 6DOF mechanism consists of 6 linear adjusters. The field lens and the CCD have their own grey triangular plates to interface the part to the adjuster mechanism.

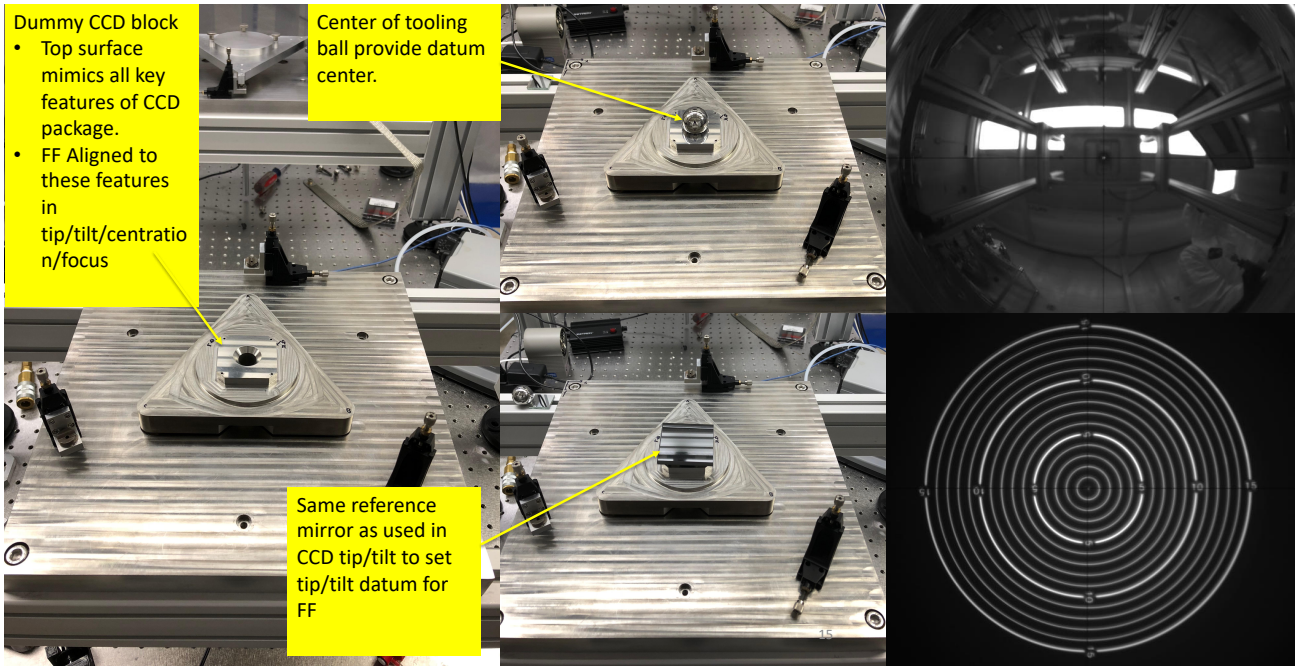

Figure 9 Datum fixtures for the field lens alignment and examples reticle target images from each datum fixture through the D-275.

Figure 9 shows the datum fixtures used for the CCD alignment. The centering datum is set by a corner cube retro reflector that is registered to the three surrogate kinematic mounting points on the alignment

platform. By setting the conjugate point of the D-275 at the center of the corner cube, we can identify the centering misalignment of the D-275 and adjust its position accordingly using the motorized adjusters of the alignment telescope. The bottom left image shows the returned reticle when the alignment telescope is aligned to the corner cube fixture in centration and clocking. The tip/tilt datum consists of a small mirror that is aligned, again to the three surrogate kinematic points on the alignment platform in tip/tilt. The alignment telescope is then adjusted to its infinity conjugate and aligned to this mirror in tip/tilt. The returned reticle image at this conjugate point is shown at the bottom right panel.

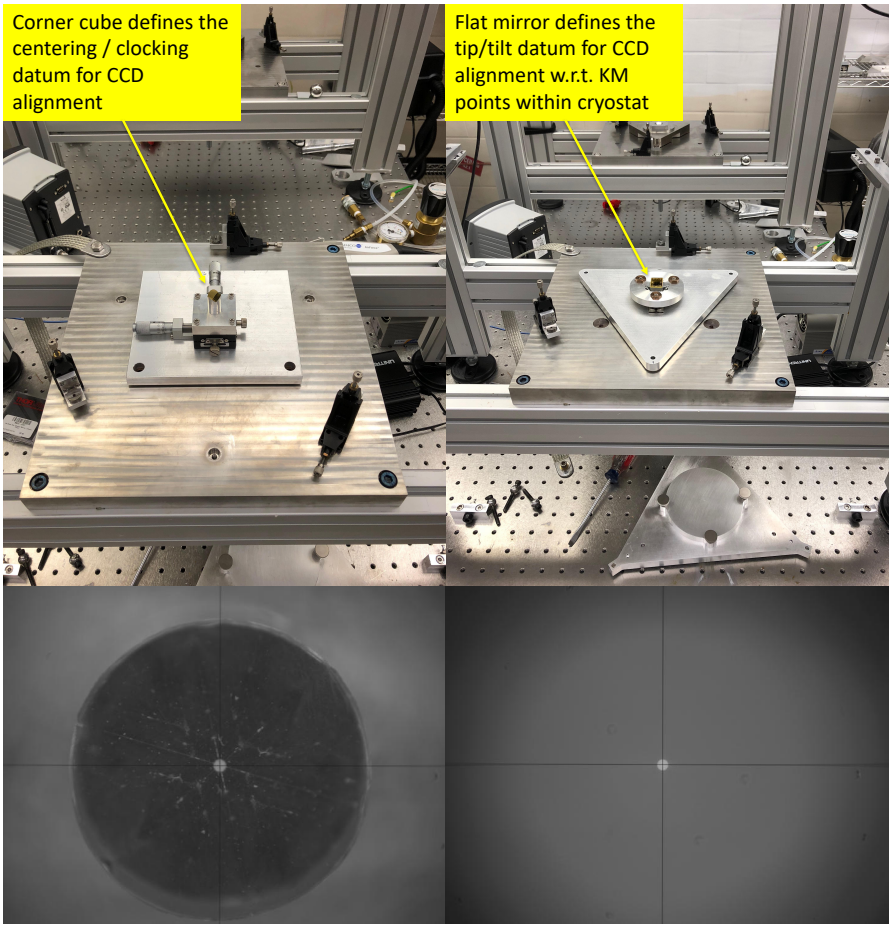

Figure 10 Datum fixtures for the CCD alignment and examples reticle target images from each datum fixture through the D-275.

6. METROLOGY STATISTICS AND EXTENSION TO MULTI-ELEMENT SYSTEM

Since the complete overhaul of the CCD-field lens alignment procedure 2 years ago, we have aligned total 65 CCD-field lens packages at the time of this writing. This corresponds to 32.5 VIRUS spectrograph units. Figure 11 shows the metrology statistics across these CCD-field lens assemblies. The table lists the final mean alignment error and 3-σ uncertainty for the field lens and CCD in all degrees of freedom. The green numbers show the expected 3-σ uncertainty range for each DOF of each part. It clearly shows that the current process is working very close to the expectation. The three plots at the bottom shows the example distributions of the field lens alignment parameters. Because the physically direct nature of the CPM technique, once the measured DOFs are within the required range, we know that the field lens and CCD assemblies met the specifications. This can be double checked by the final end-to-end optical alignment/integration of the spectrograph unit.

DOF	DX[mm]	DY[mm]	DZ[mm]	TIP[deg]	TILT[deg]	CLOCK[deg]
FF (mean)	0.001	0.003	0.001	0.001	0.001	Not constrained
FF (3-σ)	0.019 (0.018)	0.020 (0.018)	0.024 (0.020)	0.011 (0.010)	0.013 (0.010)	
CCD (mean)	0.007	0.001	0.001	0.002	0.001	0.001
CCD (3-σ)	0.024 (0.018)	0.022 (0.018)	0.021 (0.020)	0.002 (0.003)	0.003 (0.003)	0.002 (0.03)

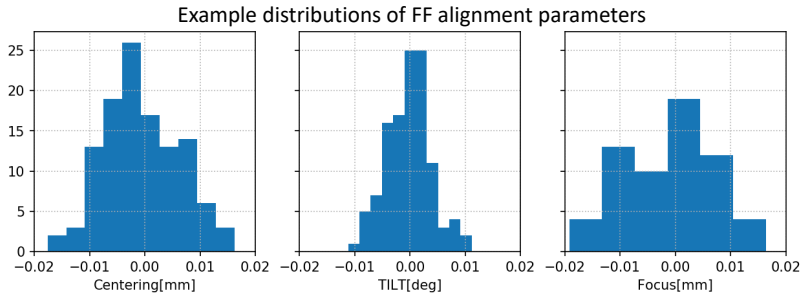

Figure 11 The optical layout of the proof-of-concept AWACS unit with two 90-deg clocked cylinder lens pair as one of two options to mimic astigmatic wavefront in the collimated air space within the unit.

Once each spectrograph unit is assembled, it undergoes an extensive fine optical alignment procedure[16][17]. In this procedure, the field aberrations of the spectrograph are measured across the CCD and the gradients in some of the major field aberrations provide the amounts and directions of the alignment compensations by the collimator mirror and the camera mirror. The CCD-field lens alignment process is needed in order to make sure that this fine optical alignment process can remove any residual aberration. This procedure is iterative, but in most of the cases it only requires one iteration. One example before-after image is shown in Figure 12 to highlight the effectiveness of this procedure.

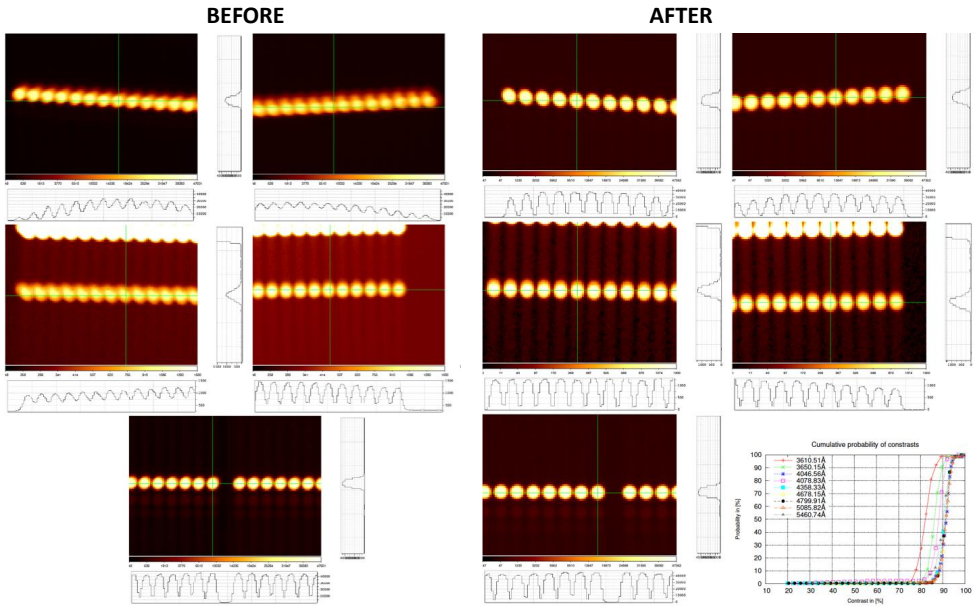

Figure 12 The fiber slit image at various places across the CCD before (left) and after (right) the fine optical alignment[17].

	CHANNEL A		CHANNEL B		
METRIC	BEFORE	AFTER	BEFORE	AFTER	UNIT
Defocus spatial gradient	0.039	0.005	0.064	0.007	wv/mm
0-Astg. spectral gradient	10.564	4.412	6.663	2.011	wv/um
COL Spatial tilt comp	0.117	0.014	0.217	0.079	degree
CAM Spatial tilt comp	0.118	0.015	0.224	0.082	degree
COL Spectral tilt comp	0.242	0.099	0.141	0.042	degree
CAM Spectral tilt comp	0.254	0.105	0.147	0.045	degree
Spatial plate scale error	n/a	0.090	n/a	0.050	%
Spectral gross dispersion error	n/a	0.100	n/a	0.100	%
Spectra positioning error	n/a	less than 4	n/a	less than 3	pixel
Constrast pass rate	0	100	0	98	%

Figure 13 The fine optical alignment metrology statistics.

Figure 13 shows the metrology statistics from the fine optical alignment of the 65 VIRUS spectrograph channels. It lists several important metrology parameters that indicate the quality of the fine optical alignment of the spectrograph units, but the most important factor among these is the one called “contrast pass rate” in the last row of the table. When the fine alignment is completed, each spectrograph channel is locked in place and then we measure the contrast across the fiber slit at different wavelengths. The peak and valley of each fiber image is then measured and the ratio between their difference and their sum is used as the contrast measure. The cutoff criterion is that the contrast must be higher than 60% for fiber images across at least 90% of the CCD area. So far, the success rate is more than 99% for the 65 VIRUS channels and this demonstrates the effectiveness of the CCD – field lens alignment / metrology procedures.

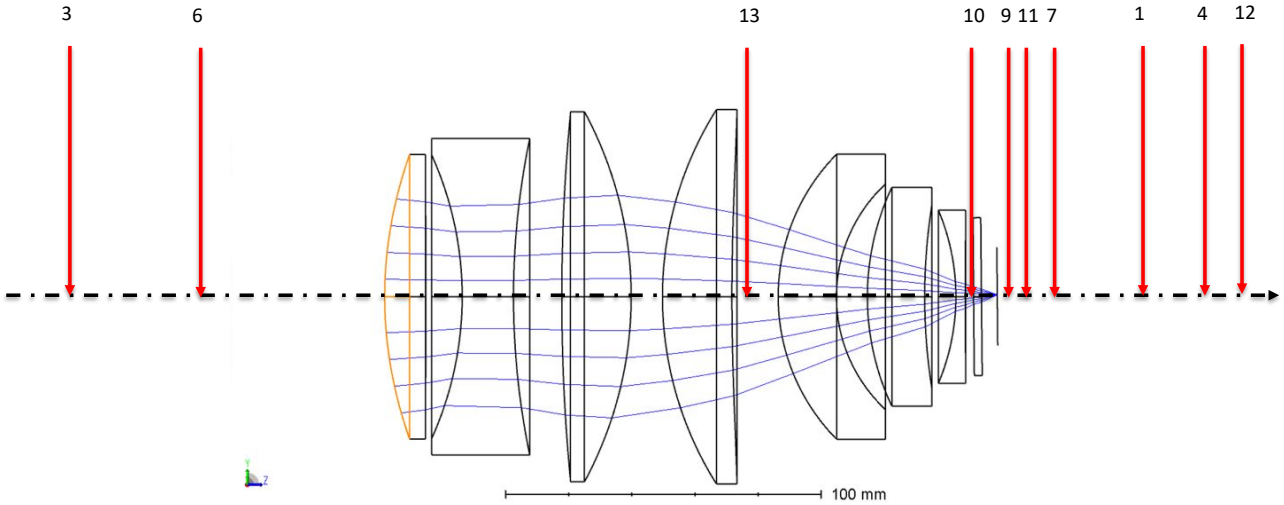

Figure 14 Example extension of the CPM technique to a multi element lens system.

Given our experience with the CPM technique, it is quite straightforward to extend it to a multi-element lens system such as shown in Figure 14. The lens system contains 7 elements with different curvatures. The key task would be to locate the conjugate points of each element. The same methodology in the VIRUS field lens alignment can be used, i.e. for each element, one can either theoretically construct the alignment sensitivity matrix using the knowledge of where each lens is roughly located with respect to the alignment telescope or empirically build it by measuring the sensitivities of the measured shifts to each of the field lens degrees of freedom. For the case of the VIRUS CCD-field lens, the empirical method was straightforward, but, for multi element system like in Figure 14, constructing it using the knowledge of the

lens locations and calibrating the sensitivity later may turn out to be more effective. However, either way will work efficiently once established.

7. SUMMARY

In this paper, we presented the conjugate point matching technique as a way to align a CCD and field lens to µm level accuracy. The principles of operations have been discussed and illustrated. We used the VIRUS spectrograph as an example to highlight various measurement process and datum set up process, and presented the metrology statistics from aligning 65 CCD-field lens assemblies. More than 99% of the assemblies and their spectrograph channels have passed the final fine optical alignment and characterizations and are currently in science operations at the HET. We briefly touched on the principle of extending the CPM technique to multi-lens systems and will continue developing this technique for the upcoming new instrument called the VIRUS2 for the Harlan J Smith Telescope at the McDonald Observatory[5].

LIST OF REFERENCES

[1] G. Hill, et al., "VIRUS: status and performance of the massively replicated fiber integral field spectrograph for the upgraded Hobby-Eberly telescope," Proc. SPIE 10702-56 (2018).

[2] A Multi Unit Spectroscopic Explorer – MUSE, https://www.eso.org/sci/facilities/develop/instruments/muse.html, European Southern Observatory.

[3] Dark Energy Spectroscopic Instrument – DESI, http://desi.lbl.gov, Lawrence Berkeley Laboratory.

[4] R. Simcoe, et al., "LLAMAS: A Facility Integral Field Spectrograph for the Magellan Telescopes," https://ait.mit.edu/sites/default/files/documents/LLAMAS_pocketguide_web.pdf.

[5] H. Lee, et al., "VIRUS-2 for the Harlan J. Smith telescope of the McDonald Observatory," Proc. SPIE 10702-307 (2018).

[6] G. J. Hill, et al., "The Hobby-Eberly Telescope Dark Energy Experiment," AIP Conference Proceedings, 773 224-223 (2004).

[7] G. Hill, et al., "Completion and performance of the Hobby-Eberly telescope wide field upgrade," Proc. SPIE, **10700-20** (2018).

[8] H. Lee, et.al, "Delivery, Installation, On-sky verification of the Hobby-Eberly Telescope wide-field corrector", Proc. SPIE, **7733**-51 (2010).

[9] B. Vattiat, et al., "Design, testing, and performance of the Hobby Eberly Telescope prime focus instrument package," Proc. SPIE 8846-72 (2012). [10][10]

[10] H. Lee, et al., "Metrology systems for the active alignment control of the Hobby-Eberly Telescope wide-field upgrade," Proc. SPIE, 9906-46 (2016).

[11] T. Chonis, et al., "LRS2: design, assembly, testing, and commissioning of the second-generation low-resolution spectrograph for the Hobby Eberly Telescope," Proc. SPIE, 9908-4C (2012).

[12] H. Lee, et al., "LRS2: a new low-resolution spectrograph for the Hobby-Eberly Telescope," Proc. SPIE, 7735-H (2010).

[13] B. Vattiat et al., "Design, assembly, and performance of the low-resolution spectrograph 2 integral field unit," Proc. SPIE 9908-3C (2016).

[14] S. Mahadevan, et al., "The Habitable-zone Planet Finder: A status update on the development of a stabilized fiber-fed near-infrared spectrograph for the for the Hobby-Eberly telescope," Proc. SPIE 91417G (2014).

[15] H. Lee, et al., "Visible Integral-field Replicable Unit Spectrograph (VIRUS) optical tolerance," Proc. SPIE 77353X (2010).

[16] H. Lee, et al., "Fine optical alignment correction of astronomical spectrographs via in-situ full-field moment-based wavefront sensing," Proc. SPIE 84500V (2012).

[17] H. Lee, et al., "Field application of moment-based wavefront sensing to in-situ alignment and image quality assessment of astronomical spectrographs: results and analysis of aligning VIRUS unit spectrographs," Proc. SPIE 91513O (2014).